X-ray Crystal Structure of a Sodium Salt of $[Gd(DOTP)]^{5-}$: Implications for Its Second-Sphere Relaxivity and the ^{23}Na NMR Hyperfine Shift Effects of $[Tm(DOTP)]^{5-}$

Fernando Avecilla,*[a] Joop A. Peters,[b] and Carlos F. G. C. Geraldes*[c]

Keywords: Gadolinium / Imaging agents / Solid-state structures / Hydration / NMR shift reagents

The X-ray structure of the sodium salt of $[Gd(DOTP)]^{5-}$ shows two different chelates, $[Gd^{(1)}(DOTP)]^{5-}$ and $[Gd^{(2)}(DOTP)]^{5-}$, bound at either surface of a sheet formed by a cluster of hydrated Na^+ ions. Each $[Gd^{(1)}(DOTP)]^{5-}$ anion binds directly to four Na^+ ions of this cluster through the free oxygen atoms of the phosphonate groups of the adjacent ligand, while each $[Gd^{(2)}(DOTP)]^{5-}$ unit is connected to the cluster via hydrogen bonds only. The Gd^{3+} ions in the two moieties do not have any inner-sphere water molecules, and are eight-coordinate. Their coordination polyhedra are twisted square antiprisms, with slightly different twist angles. These **m**′ isomers are found in the crystal structure as racemic mixtures of enantiomers. Only one set of NMR resonances is observed in aqueous solution, corresponding to an averaged **m**′ isomer. In this crystal structure, the Na^+ ions bind the phosphonate oxygen atoms of the $[Gd^{(1)}(DOTP)]^{5-}$ anion at positions far removed from the main symmetry axis. This is significantly different from the binding mode(s) previously proposed to be occurring in solution between Na^+ and $[Tm(DOTP)]^{5-}$, based on the interpretation of solution paramagnetic ^{23}Na NMR shifts. This could arise as a result of the effects of the cluster of hydrated Na^+ ions that are present, which may hinder axial binding modes and distort lateral binding modes. Further, in the crystal structure, both types of Gd^{3+} centers have four second-sphere water molecules that are located at distances (4.2–4.5 Å) significantly longer than those previously proposed from the analysis of the NMRD data of $[Gd^{(1)}(DOTP)]^{5-}$. This is a result of the coordination of Na^+ by these water molecules, thus preventing their direct interaction with the phosphonate oxygen atoms. However, in solution such second-sphere water molecules can interact strongly with the phosphonate ligand oxygen atoms, resulting in efficient relaxation if their binding has relatively long lifetimes (> 50 ps). Rotational immobilization will amplify this contribution, thus making it similar to outer-sphere relaxation.

Introduction

Stable lanthanide chelates of polyazamacrocyclic ligands have been widely used as paramagnetic shift reagents for the in vivo NMR spectroscopy of cations,[1] and as contrast agents for magnetic resonance imaging (MRI).[2–5] The Tm^{3+} complex of 1,4,7,10-tetraazacyclododecane-1,4,7,10-tetrakis(methylenephosphonic acid) (H_8DOTP) has proved to be a particularly favorable NMR shift reagent for the $^{23}Na^+$ NMR spectroscopic study of isolated cells,[6] perfused tissues,[7–11] and intact animals.[12–15] It is also useful as an extracellular in vivo marker of tissues.[16,17] The relaxation properties of the Gd^{3+} complex, $[Gd(DOTP)]^{5-}$, a potential MRI contrast agent, have also been studied.[18–20] Although the solution structures of the Ln^{3+} complexes of this ligand[21–24] have been thoroughly investigated using multinuclear NMR spectroscopic techniques by exploiting the structural information content of the paramagnetic effects of these ions,[25,26] only a preliminary X-ray crystal structure of the $[(NH_4)_5Tm(DOTP)]$ complex has been reported.[27] Here we report on the single-crystal X-ray structural determination of $[Na_5Gd(DOTP)]$. The structural data are used to compare the configuration of the bound ligand with that found in solution.[22] The binding of the Na^+ ions and the positions of the water molecules found in this crystal structure are compared with what has been proposed in solution from ^{23}Na NMR spectroscopic[28,29] and relaxivity studies.[18–20]

[a] Departamento de Química Fundamental, Universidade da Coruña,
Campus de A Zapateira s/n, 15071 A Coruña, Spain
[b] Laboratory for Applied Organic Chemistry and Catalysis, Delft University of Technology,
Julianalaan 136, 2628 BL Delft, The Netherlands
[c] Departamento de Bioquímica, Faculdade de Ciências e Tecnologia, Universidade de Coimbra,
Apartado 3126, 3049 Coimbra, Portugal
Fax: (internat.) + 351-239/853607
E-mail:geraldes@ci.uc.pt
Supporting information for this article is available on the WWW under http://www.eurjic.org or from the author.

Results and Discussion

X-ray Crystal Structure of the Na^+ Salt of $[Gd(DOTP)]^{5-}$

The chemical formula of the compound in the crystal form, as obtained from the X-ray diffraction crystal structural analysis, is $[\{Na_{13}(OH)_3(H_2O)_{29}\}\{Gd^{(1)}(DOTP)\}][Gd^{(2)}(DOTP)]\cdot 7H_2O\cdot 2CH_3CH_2OH$. The overall structure of the crystal is shown in Figure 1, where the asymmetric unit contains two different $[Gd(DOTP)]^{5-}$ moieties, with the $Gd^{(1)}$ and $Gd^{(2)}$ atoms as centers. Within this unit, there are 0.25 $Gd^{(1)}(DOTP)$ moieties, 3.25 Na^+ ions, 0.75 hydroxide groups and 7.25 water molecules that form a hydrated Na^+ cluster. $Gd^{(2)}$ also contributes to the asymmetric unit with an isolated quarter of $Gd^{(2)}(DOTP)$, in which the oxygen atoms of its phosphonate groups are directed to the hydrated Na^+ cluster. 1.75 water and 0.5 ethanol molecules of crystallization complete the structure. This basic unit is repeated according to the crystal symmetry, with the formation of the complete structure.

The $[Gd^{(1)}(DOTP)]^{5-}$ anion, along with the associated Na^+ ions and water molecules is presented in more detail in Figure 2. Four Na^+ ions [Na(4)] are coordinated directly to $[Gd^{(1)}(DOTP)]^{5-}$, each Na^+ ion forms a bridge between the two Gd^{3+}-unbound oxygen atoms of the phosphonate groups of the adjacent ligand. One of these oxygen atoms points towards the azamacrocycle, while the other points towards a cluster of hydrated Na^+ ions that is located next to the methylenephosphonate pendant arms of the macrocycle, connected to the four phosphonate-bound Na^+ ions through four bridging water molecules. The sodium ions are either eight-coordinate [e.g. Na(2)], as in the center of the cluster, six-coordinate at the edges of the cluster [e.g. Na(1)], or four-coordinate when bound to the oxygen atoms of the ligand phosphonate groups [Na(4) in Figure 2]. There are no water molecules directly coordinated to the $[Gd^{(1)}(DOTP)]^{5-}$ moiety. The $[Gd^{(2)}(DOTP)]^{5-}$ anion can also be seen in detail in Figure 2. Although there are many water molecules in the vicinity of the Na^+ ions, no water molecule is directly coordinated by the $[Gd^{(2)}(DOTP)]^{5-}$ chelates. The isolated $[Gd^{(2)}(DOTP)]^{5-}$ unit is connected via hydrogen-bond interactions to the hydrated $[\{Na_{13}(OH)_3(H_2O)_{29}\}\{Gd^{(1)}(DOTP)\}]$ cluster. Table 1 lists some selected interatomic distances. The close proximity of O(1W) to the O(4) and O(5) atoms may indicate a hydrogen-bond between these atoms. The calculated values for the O(1W)···O(4) and O(1W)···O(5) distances, 2.860(13) and 2.966(14), and the angles O(1W)H(1W1)···O(4) and O(1W)H(1W2)···O(5), 169.0 and 149.4°, respectively, fall within the expected ranges.

The molecular geometries of the $[Gd^{(1)}(DOTP)]^{5-}$ and $[Gd^{(2)}(DOTP)]^{5-}$ anions are shown in Figure 3. The Gd^{3+} ion is eight-coordinate, four nitrogen atoms of the macrocycle and four phosphonate oxygen atoms of the pendant arms are bound by it. No inner-sphere water molecule is coordinated by the center. The coordination polyhedra around the Gd^{3+} ions can be described as a twisted intermediate between a prism and a square antiprism. A geometric analysis of the structure was performed in order to

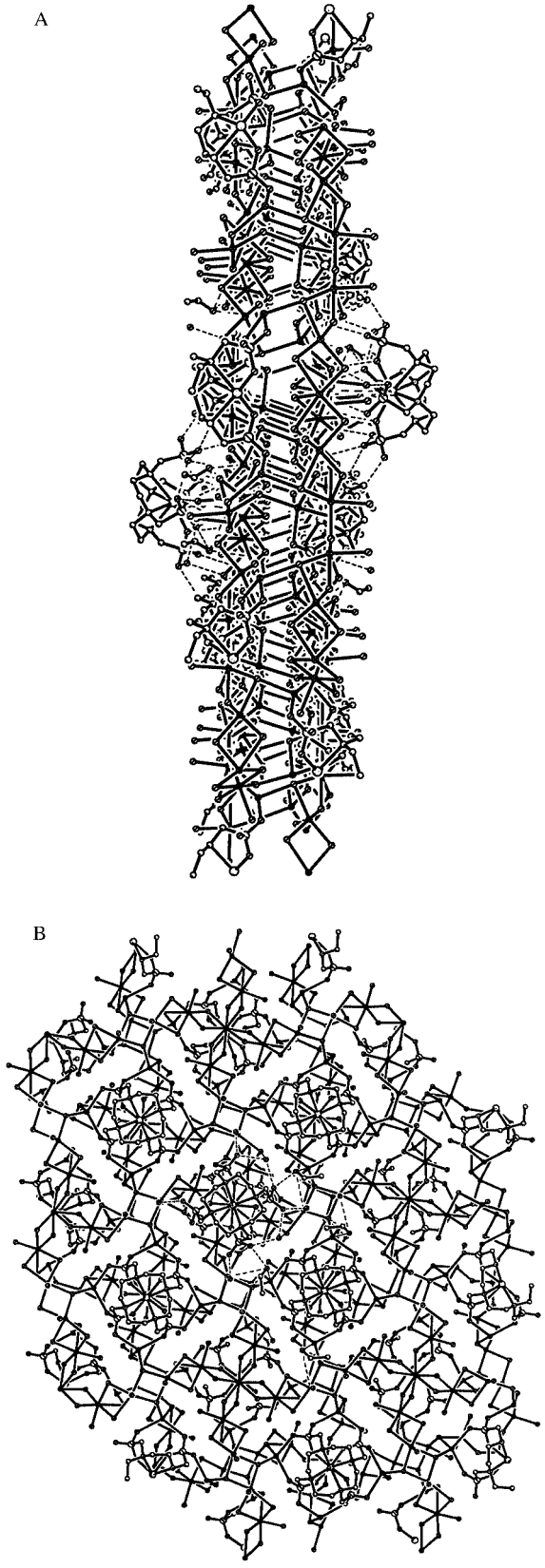

Figure 1. Packing views of the crystal structure of $[\{Na_{13}(OH)_3(H_2O)_{29}\}\{Gd^{(1)}(DOTP)\}][Gd^{(2)}(DOTP)]\cdot 7H_2O\cdot 2CH_3CH_2OH$; the cluster of hydrated Na^+ ions is shown in the middle of two layers in parallel planes perpendicular to the axis connecting $Gd^{(2)}$ and $Gd^{(1)}$: (A) side view; (B) top view

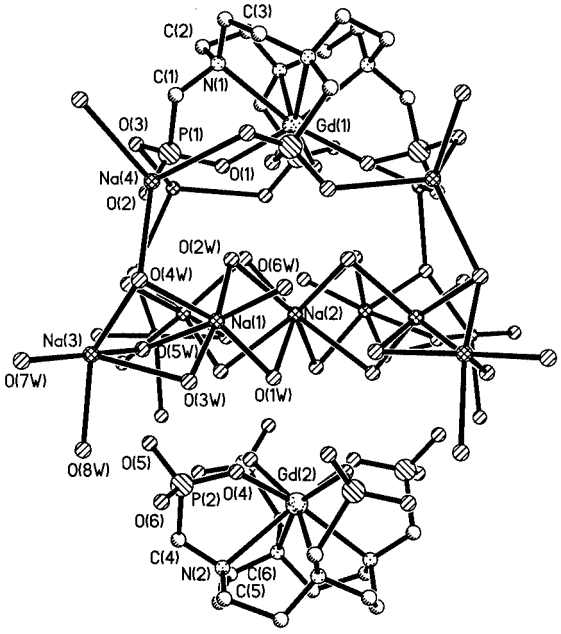

Figure 2. A general view of the supramolecule in the solid state, including the external spheres of the $[Gd^{(1)}(DOTP)]^{5-}$ and $[Gd^{(2)}(DOTP)]^{5-}$ moieties; hydrogen atoms are omitted for simplicity

Table 1. Selected interatomic distances [Å] for $[\{Na_{13}(OH)_3(H_2O)_{29}\}\{Gd^{(1)}(DOTP)\}]\,[Gd^{(2)}(DOTP)]\cdot 7H_2O\cdot 2CH_3CH_2OH$

Gd(1)−O(1)	2.312(6)	Gd(2)−O(4)	2.314(9)
Gd(1)−N(1)	2.652(10)	Gd(2)−N(2)	2.667(16)
P(1)−O(1)	1.533(7)	P(2)−O(4)	1.492(10)
P(1)−O(2)	1.545(10)	P(2)−O(5)	1.525(12)
P(1)−O(3)	1.486(9)	P(2)−O(6)	1.473(12)
P(1)−C(1)	1.842(15)	P(2)−C(4)	1.904(15)
Na(1)−O(1 W)	2.377(9)	Na(3)−O(3 W)	2.691(18)
Na(1)−O(2 W)	2.360(11)	Na(3)−O(4 W)	2.325(15)
Na(1)−O(3 W)	2.367(14)	Na(3)−O(5 W)	2.414(10)
Na(1)−O(4 W)	2.625(17)	Na(3)−O(7 W)	2.387(11)
Na(1)−O(5 W)	2.425(10)	Na(3)−O(8 W)	2.44(2)
Na(1)−O(6 W)	2.413(10)	Na(4)−O(2)	2.700(12)
Na(2)−O(1 W)	2.671(11)	Na(4)−O(3)	2.842(14)
Na(2)−O(2 W)	2.664(11)	Na(4)−O(4 W)	2.744(15)
		Na(4)−O(7 W)	2.743(14)

determine the degree of torsion of the prism around the pseudo C_4 axis.[30] The resulting geometry of the coordinated atoms is almost midway between prismatic (twist angle between the planes: 0°) and antiprismatic (twist angle: 45°). Negative twist angles of −27.07 and −23.67° are found in the structures for $[Gd^{(1)}(DOTP)]^{5-}$ and $[Gd^{(2)}(DOTP)]^{5-}$, respectively, which can both be defined as eight-coordinate twisted (or inverted) square-antiprismatic (TSAP) structures, also known as **m′** isomers.[31a] A twisted antiprismatic structure has also been reported for $[La(DOTA)]^-$ crystals: a nine-coordinate twisted capped square-antiprismatic (TCSAP) structure with a twist angle of about −22°, and a water molecule at the capping position.[31b] The two slightly different twist angles observed for the two types of $[Gd(DOTP)]^{5-}$ chelates probably result from their different interactions with the cluster of hydrated Na^+ ions in the crystal structure, and have not been reported in a previous preliminary crystal structural study.[27]

The inherent structural features of the $[Gd(DOTP)]^{5-}$ chelate give rise to two independent sources of chirality, associated with the conformation of each of the four Gd-NCCN chelate moieties in the macrocyclic ring (the helicity of the four C−C bonds relative to the respective Gd^{3+}−N−N planes is defined by two possible forms, δ and λ) and the helicity of the pendant arms (Δ or Λ).[26] The two twisted square-antiprismatic **m′** isomers found in the crystal structure appear both as racemic mixtures of the two Δ(δ,δ,δ,δ) and Λ(λ,λ,λ,λ) enantiomers.

In the coordination polyhedra, the Gd−N bond lengths are 2.660(1) Å (ave.) and the Gd−O bond lengths are 2.314(8) Å (ave.), while in the twisted square-antiprismatic Tm^{3+} coordination polyhedron of $[(NH_4)_5Tm(DOTP)]$, the Tm−N bond lengths were found to be 2.63(1) Å (ave.) and the Gd−O bond lengths 2.26(1) Å (ave.).[27]

These solid-state structural data agree with the results of the solution structural studies on the $[Ln(DOTP)]^{5-}$ complexes carried out using multinuclear and paramagnetic NMR spectroscopy.[21−24] ^{17}O NMR spectroscopic measurements of $[Dy(DOTP)]^{5-}$ in solution have shown that this complex lacks an inner-sphere water molecule.[23] The diamagnetic $[La(DOTP)]^{5-}$ and $[Lu(DOTP)]^{5-}$ complexes have been studied by ^1H and ^{13}C NMR spectroscopy, while the complete paramagnetic series of the $[Ln(DOTP)]^{5-}$ complexes has been studied by ^1H, ^{13}C, ^{31}P, and ^{23}Na NMR spectroscopy, as well as molecular mechanics calculations.[22] Unlike DOTA complexes, which appear in solution as enantiomeric pairs of nine-coordinate capped square-antiprismatic (CSAP, also called **M**) and twisted capped square-antiprismatic (TCSAP, also called **m**) isomers,[25,26,31a] $[Ln(DOTP)]^{5-}$ complexes exist in solution as a single enantiomeric pair. Although the coordination cage appears to be locked into a single conformation, variable-temperature ^1H and ^{13}C NMR spectra suggested dynamic behavior related to the interconversion of the ethylenediamine chelate rings, coupled with the concerted flipping motion of the arms. As a result, $[Ln(DOTP)]^{5-}$ complexes exist as racemic mixtures in solution, and the two enantiomers give indistinguishable NMR signals at room temperature when using conventional NMR spectroscopic techniques.[22,23] Structural analysis of the dipolar contribution to the LIS values and MMX force-field calculations initially suggested a distorted square-antiprismatic (SAP) **M′** arrangement of the ligand, with only minor structural changes throughout the Ln series.[22] However, a recent re-evaluation of the data and of the assignments of the methylenephosphonate protons led to the conclusion that the enantiomeric pair present in solution corresponds to a twisted square-antiprismatic (TSAP) **m′** structure.[32] Thus, the two slightly different **m′**-type enantiomeric pair structures observed in the solid state are replaced by just one pair in solution, as the interaction between the $[Gd(DOTP)]^{5-}$ chelates and the cluster of the hydrated Na^+ ions breaks down

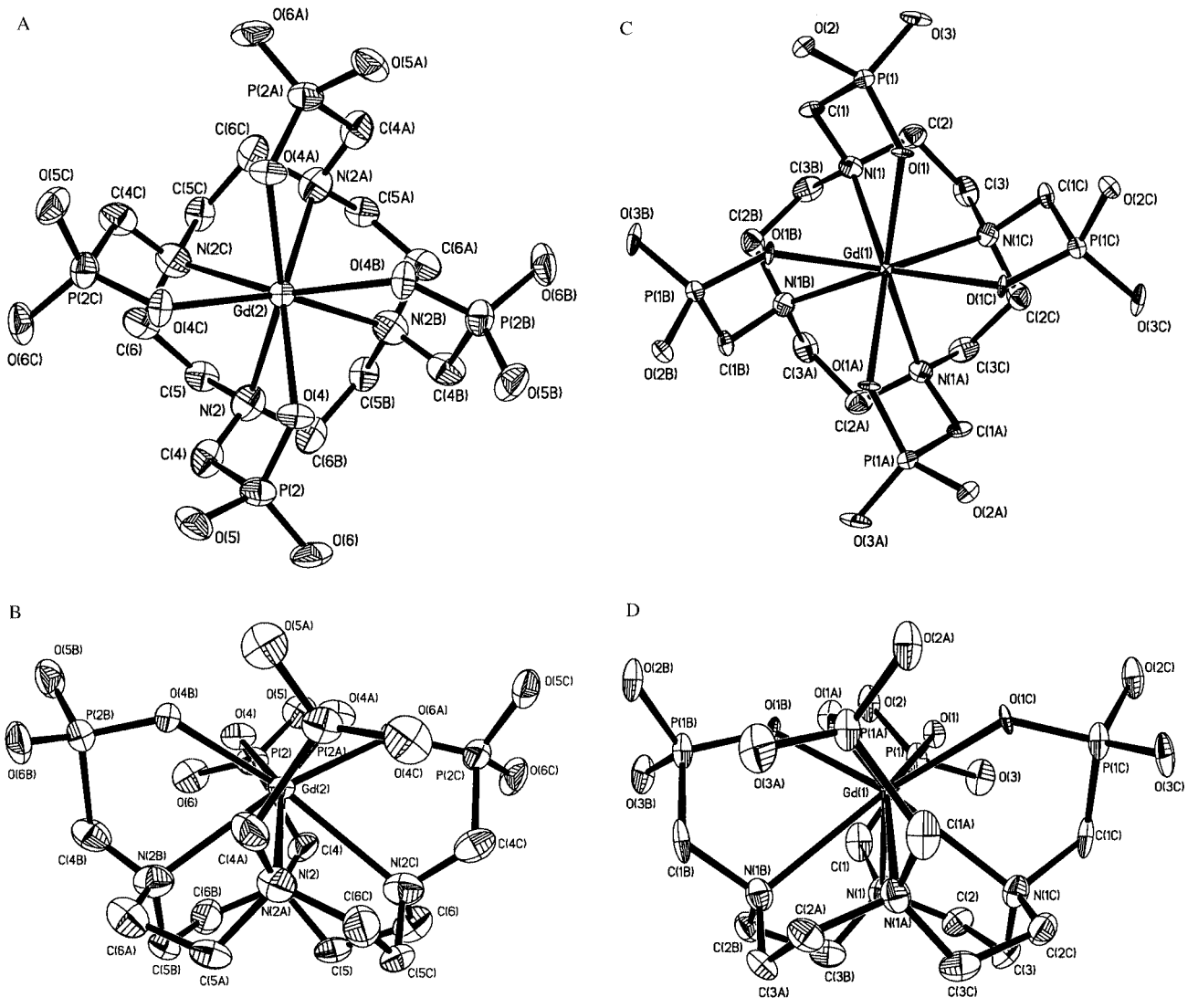

Figure 3. ORTEP diagrams with the top (A, C) and side (B, D) views of the anion complexes $[Gd^{(2)}(DOTP)]^{5-}$ (A, B) and $[Gd^{(1)}(DOTP)]^{5-}$ (C, D), representing the two square-antiprismatic **m**′ isomers; hydrogen atoms have been omitted for simplicity, the ORTEP plots are at the 30% probability level

in solution. Chiral NMR resolution, using the formation of diastereomeric adducts between the two enantiomers of $[Ln(DOTP)]^{5-}$ and a chiral substrate, has provided indirect, but conclusive, evidence for the existence of the two enantiomers of **m**′ in solution.[33−36]

Structural Evaluation of the $[Tm(DOTP)]^{5-}$-Induced ^{23}Na NMR Shifts

The magnitudes of the solution ^{23}Na LIS induced by $[Ln(DOTP)]^{5-}$ complexes, in particular by $[Tm(DOTP)]^{5-}$, are very large and are most likely due to the formation of strong ion-pairs resulting from the high negative charge on the DOTP complexes. Consequently, $[Tm(DOTP)]^{5-}$ is a very efficient shift reagent for in vivo $^{23}Na^+$ NMR spectroscopic studies. The binding sites of the Na^+ ions found in the present crystal structure of the Na^+ salt of $[Gd(DOTP)]^{5-}$ can be used to check the interpretation of the ^{23}Na LIS induced in solution by $[Tm(DOTP)]^{5-}$.[28,29] In this solid-state structure, the $[Gd^{(1)}DOTP)]^{5-}$ center displays four Na^+ ions [Na(4)] that are directly coordinated to the bound ligand and that form bridges between two Gd^{3+}-unbound oxygen atoms of the phosphonate groups of the adjacent ligand (Figure 2). The experimental structural parameters of this binding mode are $\theta = 72.6°$ and $r = 5.29$ Å, where θ is the angle between the four-fold symmetry axis of the $[Gd(DOTP)]^{5-}$ moiety and the $Gd^{3+}-Na^+$ vector, and r is the $Gd^{3+}-Na^+$ distance. The $[Gd^{(2)}(DOTP)]^{5-}$ moiety has no Na^+ ions directly coordinated to the bound ligand (Figure 2), but several of them can be found in its vicinity that belong to the hydrated Na^+ cluster. These ions form two layers in parallel planes perpendicular to the axis

connecting $Gd^{(2)}$ and $Gd^{(1)}$, which is the main susceptibility axis of $Gd^{(2)}$. Five Na^+ ions can be found in a layer further away from $Gd^{(2)}$.

Two different types of binding sites for the Na^+ counterions have been proposed in order to interpret the solution ^{23}Na LIS induced by $[Tm(DOTP)]^{5-}$.[28,29] The extremely large ^{23}Na LIS (ca. 420 ppm) observed at low $Na^+/[Tm(DOTP)]^{5-}$ ratios was interpreted as resulting from a type of binding (type A) at a position near the four-fold symmetry axis (low θ). In particular, MMX calculations generated an optimal model where the Na^+ ion interacts with one Tm-bound oxygen atom and another oxygen atom of an adjacent phosphonate group which points away from the tetraazamacrocycle (model A_4, with dipolar angle θ = 26°, $Tm^{3+}-Na^+$ distance r = 3.78 Å).[29] The much smaller shifts (ca. 160 ppm) observed at high $Na^+/[Tm(DOTP)]^{5-}$ ratios were interpreted as resulting from four binding sites of a second type (type B) at higher θ and r values. An MMX-optimized model suggested that the Na^+ ions are associated with two unbound oxygen atoms of adjacent phosphonate groups that point away from the tetraazamacrocycle, with an average θ = 36°, and r = 4.56 Å (model B_2).[29] Both proposed binding sites are located within the positive shift cone of the lanthanide ion.

The structural parameters of the four $Na^+(4)$ ions bound to the $[Gd^{(1)}(DOTP)]^{5-}$ moiety in the crystal show that this binding is similar to the second proposed (type B) binding mode (model B_2), rather than to the first (type A), but with a much larger angle θ (θ > 54.5°) and distance r, thus, the Na^+ ions are located in the negative shift cone of the lanthanide ion. This would lead to a small negative ^{23}Na LIS value for $[Tm(DOTP)]^{5-}$, thereby contradicting the NMR spectroscopic data.[6−15] The $Na^+(4)$ binding mode is very similar to the B_3 model (Na^+ binding to the two oxygen atoms of the same phosphonate group), which has not been considered to contribute to the experimental ^{23}Na LIS.[28,29]

The Na^+ ions in the cluster, near the $[Gd^{(2)}(DOTP)]^{5-}$ moiety but not directly bound to it, occupy three different types of sites. One Na^+ ion [Na(2), θ = 0°, r = 5.17 Å] is located along that susceptibility axis of $Gd^{(2)}$, thus at equal distances from the four phosphonate moieties. It occupies a type-A position, but at a significantly larger distance than the proposed binding model A_1 (θ = 0° and r = 3.22 Å). Four Na^+ ions [Na(1), θ = 36.7°, r = 6.37 Å] occupy a type-B position, but at a larger distance than model B_1, and coordinate one of the metal-unbound oxygen atoms of one bound phosphonate group (θ = 36.7°, r = 5.42 Å). Another four Na^+ ions [Na(3), θ = 56.6°, r = 7.92 Å], which are part of the layer closer to $Gd^{(2)}$, are located at wider angles from the main axis and at larger distances from $Gd^{(2)}$; a position that is similar to the binding model B_3 (θ = 65.5°, r = 6.05 Å), but also at a larger distance.[29]

Therefore, from this analysis we can conclude that the Na^+ binding sites detected in the crystal structure of the Na^+ salt of $[Gd(DOTP)]^{5-}$ at a high $Na^+/[Gd(DOTP)]^{5-}$ ratio of 5 do not represent the binding mode(s) previously proposed to be occurring in solution. This could arise as a result of the effects of the cluster of hydrated Na^+ ions that are present, which may hinder the axial binding mode (type A) and also distort the lateral binding mode (type B).

Simulation of the Parameter Dependence of the Second-Sphere and Outer-Sphere Contributions to the Relaxivity of a Gd^{3+} Complex

The unexpectedly high relaxivities displayed by the NMRD profiles of some small Gd^{3+} chelates such as $[Gd(DOTP)]^{5-}$,[18,19] and also of some small Gd^{3+} chelates bound to macromolecules such as HSA,[37−43] led to the proposal that second-sphere water molecules may, in some cases, significantly contribute to the measured relaxivities.[43−45] Such second-sphere relaxivity contributions could become as important as well-recognized outer-sphere contributions. The Solomon−Bloembergen−Morgan equations, which usually describe the field dependency of the inner-sphere relaxivity, can be adapted to describe second-sphere effects, while Freed's equation is used to describe the outer-sphere contribution of the relaxivity.[46] Both equations depend on a variety of molecular parameters. In order to obtain an insight into the factors that determine the relative importance of both contributions, the values of the second-sphere and outer-sphere relaxivities of the water protons of a Gd^{3+} complex in aqueous solution were simulated at 298 K and at the 0.01 MHz and 40 MHz Larmor frequencies, as a function of various relevant parameters. The set of equations used is given in the Supporting Information.

Second-sphere relaxivity depends on a variety of parameters, some of which were fixed at reasonable values, such as the number of second-sphere water molecules (q' = 1) and the electronic relaxation parameters ($\Delta^2 = 6.94\cdot10^{19}$ s^2, τ_v = 15 ps). The distance (r') from Gd^{3+} to a second-sphere water proton was varied between two reasonable values, 3.5 and 3.9 Å, while its exchange lifetime $\tau_{M'}$ was varied between 10 and 100 ps, assuming fast (τ_R = 50 ps) and slow ($\tau_R = 10^4$ ps) rotational diffusion of the complex. The outer-sphere contribution has been simulated before as a function of the distance of closest approach of a water molecule to Gd^{3+} (a^H), the diffusion constant (D) and the electronic relaxation time at zero field (τ_{S0}), which is a function of the crystal-field parameter Δ^2.[47] Here, the outer-sphere contribution was calculated as a function of the parameter a^H, which took on the values of 3.5, 3.9, and 4.5 Å, with the same electronic relaxation parameters as assumed for second-sphere relaxation and a typical value of the diffusion constant, $D = 2.28\cdot10^{-9}$ $m^2\cdot s^{-1}$. These simulations (Figure 4) show that the second-sphere relaxation is efficient only if the second-sphere water molecules have a reasonably long lifetime $\tau_{M'}$. In such a case, rotational immobilization (long τ_R) may amplify this contribution, so that it becomes similar to outer-sphere relaxation. Thus, the long-lived second-sphere hydration water molecules trapped in the interface of a Gd^{3+} chelate binding at a pocket of a protein such as HSA, together with exchangeable protons from protein residues nearby, have very sizeable contributions to the large relaxivities observed.[5,43]

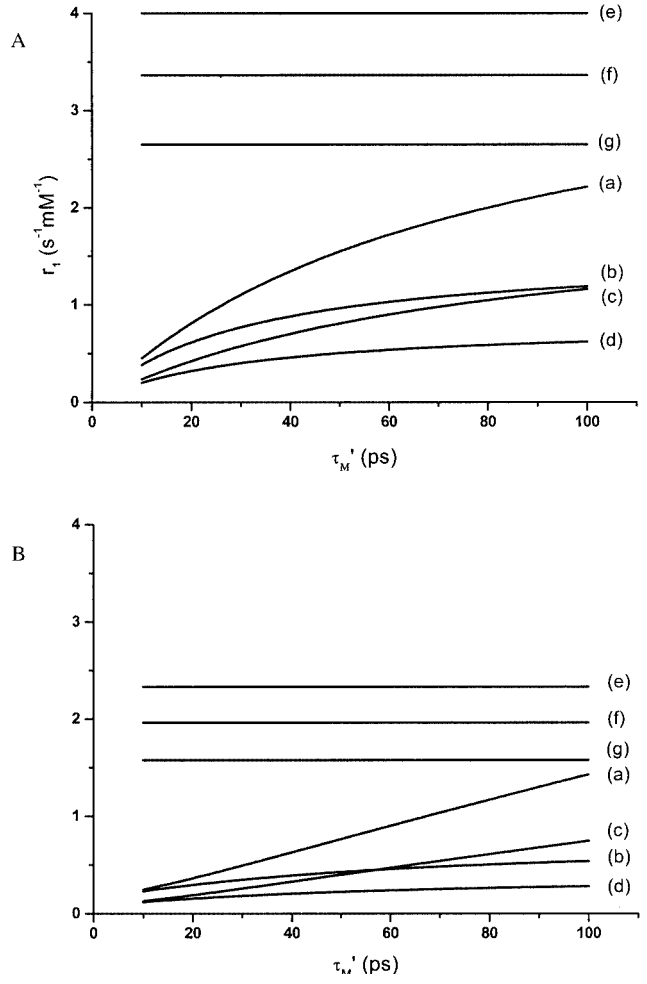

Figure 4. Calculated values at 0.01 MHz (A) and 40 MHz (B) of the parameter dependencies of the contributions to the proton relaxivity r_1 of a Gd^{3+} complex in aqueous solution: (a)−(d) second-sphere relaxivity as a function of $\tau_{M'}$ for $\tau_R = 50$ ps, $r' = 3.5$ Å (b) and $r' = 3.9$ Å (d) and for $\tau_R = 10^4$ ps, $r' = 3.5$ Å (a) and $r' = 3.9$ Å (c) ($q' = 1$, $\Delta^2 = 6.94 \cdot 10^{19}$ s^2, $\tau_v = 15$ ps); (e)−(g) outer-sphere relaxivity for $a^H = 3.5$ Å (e), $a^H = 3.9$ Å (f), and $a^H = 4.5$ Å (g) ($D = 2.28 \cdot 10^{-9}$ $m^2 \cdot s^{-1}$, $\Delta^2 = 6.94 \cdot 10^{19}$ s^2, $\tau_v = 15$ ps)

Structural Evaluation of the Second-Sphere Hydration of Gd^{3+} in $[Gd(DOTP)]^{5-}$ and of Its Contribution to Its Relaxivity

The NMRD profile of $[Gd(DOTP)]^{5-}$ shows a relatively high relaxivity,[18,19] and its unusual features have led to conflicting explanations. Initially, the formation of oligomers containing a mixture of isomers with different q (inner-sphere water molecules) values were considered, leading to fractional q values.[18] Later, the same curve was interpreted on the basis of the collective contributions of one coordinated water molecule ($q = 1$) with an unusually long distance, $r_{GdH} = 3.26$ Å (instead of the standard 2.9 Å value) and a residence time, $\tau_M = 3000$ ps, together with an outer-sphere contribution calculated using a rather short distance of closest approach $a_{GdH} = 3.76$ Å,[19,20] instead of the more commonly used value of $a_{GdH} = 4.5$ Å.[44] As it became evident that this system has $q = 0$,[23] the same data were well-fitted when considering a strong second-sphere contribution, with two water molecules ($q' = 2$) located at a somewhat longer distance ($r'_{GdH} = 3.89$ Å) with short residence times ($\tau'_M \approx 100$ ps), corresponding to water molecules hydrogen-bonded to the phosphonate oxygen atoms of $[Gd(DOTP)]^{5-}$, together with an outer-sphere contribution calculated using standard values of D and $a_{GdH} = 4.5$ Å.[45] The important contribution of second-sphere water molecules to the relaxivity of $[Gd(DOTP)]^{5-}$ was also pinpointed by a reasonable fit of its NMRD curve to a calculated curve based on an outer-sphere hydration model obtained by molecular dynamics simulations. This hydration model was defined by a radial distribution function which contains a second-sphere of four water molecules on the hydrophilic hemisphere encasing the phosphonate groups of the complex, at an average distance $r'_{GdH} = 3.4$ Å, and residence time $\tau'_M = 56$ ps.[48]

We tried to find experimental evidence of the solution hydration model of $[Gd(DOTP)]^{5-}$ from the low-temperature (−100 °C) X-ray structure, in a similar way to what was done previously for $K_2[Yb(DTPA)(H_2O)]$.[44] However, this was not as successful since the presence of the Na^+ counterions in close contact with the complex (Figure 2) significantly affects its hydration. Eight water molecules that are coordinated to the four Na^+ ions, which are bound to the phosphonate groups, are at 7.0−7.3 Å away from $Gd^{(1)}$. Half of these connect the four Na^+ ions to the main hydrated Na^+ cluster. Another four water molecules belonging to the cluster that connect the $Na^+(1)$ and $Na^+(2)$ ions are at 4.5 Å from $Gd^{(1)}$. The $[Gd^{(2)}DOTP]^{5-}$ chelates interact with the hydrated Na^+ cluster through the hydrogen-bonding interaction between one Gd-unbound oxygen atom of each phosphonate group and a water molecule that is coordinated to the $Na^+(3)$ ions of the cluster. These water molecules are located 7.0 Å from $Gd^{(2)}$. However, the layer of eight water molecules within the cluster are closer to $Gd^{(2)}$: four water molecules at 4.2 Å from $Gd^{(2)}$, which connect the $Na^+(1)$ and $Na^+(2)$ ions, and four water molecules at 6.7 Å from $Gd^{(2)}$, which connect the two $Na^+(1)$ and $Na^+(3)$ ions. Thus, in the crystal structure, both the $Gd^{(1)}$ and $Gd^{(2)}$ centers have four second-sphere water molecules located at 4.5 and 4.2 Å, respectively, from them. These distances are significantly longer than those proposed from the analysis of NMRD data.[45,48] The water molecules in the crystal coordinate the Na^+ ions, which prevents their direct interaction with the phosphonate oxygen atoms, significantly increasing their distances from the Gd^{3+} ions.

In summary, the structural information obtained in the solid state for the Na^+ salt of $[Gd(DOTP)]^{5-}$ provides significant clues to the location of Na^+ ions and water molecules around the chelate, which are of value for the rationalization of the solution ^{23}Na paramagnetic NMR shifts induced by $[Tm(DOTP)]^{5-}$, and of the second-sphere water relaxivity of $[Gd(DOTP)]^{5-}$.

Experimental Section

X-ray Crystallographic Study: $Na_5Gd(DOTP) \cdot 2.75\ H_2O$ was provided by Macrocyclics, Richardson, Texas, USA. Single crystals of

$[\{Na_{13}(OH)_3(H_2O)_{29}\}\{Gd^{(1)}(DOTP)\}][Gd^{(2)}(DOTP)]\cdot 7H_2O\cdot 2CH_3CH_2OH$ were recrystallized from a water/ethanol solution of the sodium salt of $[Gd(DOTP)]^{5-}$ and grown by slow diffusion of 2-propanol into this solution, and slow evaporation of the solvent. Colorless crystals of X-ray quality were obtained. A suitable crystal of $[\{Na_{13}(OH)_3(H_2O)_{29}\}\{Gd^{(1)}(DOTP)\}][Gd^{(2)}(DOTP)]\cdot 7H_2O\cdot 2CH_3CH_2OH$ was coated with Fomblin oil, placed on the end of a silica fiber and mounted on a goniometer head of a Bruker SMART CCD diffractometer with a stream of cold nitrogen gas. The crystal was centered optically, and the unit cell parameters and an orientation matrix for data collection were obtained at −100 °C by using the centering program in the SMART system. Details of the crystal data are given in Table 2. The default hemisphere runs required about 3.5 h for full data collection (with 5-s-per-frame scan time) and comprised 3 runs totaling about 1250 frames. They were set up assuming a sample-to-detector distance of about 5 cm, which provided full coverage to better than 0.75 Å (56.6° with Mo radiation). Three-dimensional X-ray data were collected by 3-circle hemisphere runs in the θ-range method. Lorentz, polarization and decay corrections were applied to the data, as well as an absorption correction based on a series of ψ scans. Reflections were measured from a hemisphere of data collected in frames of 0.3°. A total of 35498 reflections was collected, of which 4568 independent reflections exceeded the significance level $|F|/\sigma(|F|) > 4.0$. Complex scattering factors were taken from the program package SHELXTL/PC V5.1.[49] The structure was solved by direct methods and refined by full-matrix least-squares methods on F^2 using SHELXTL/PC V5.1.[49] Due to the crystal nature and diffraction capabilities, some disagreeable reflections were suppressed. All non-hydrogen atoms were refined anisotropically. Hydrogen atoms were included in calculated positions and refined with the riding model on their respective heteroatoms, except for the H atoms involved in hydrogen-bonding interactions with the $[Gd^{(2)}(DOTP)]^{5-}$ moieties, which were first located in geometrically calculated positions, left freely and then refined riding on the oxygen atoms of the water molecules. The H atoms of some water molecules and of the ethanol molecule were not included. Minimum and maximum final electron-densities (−1.571 and 3.976 e·Å^{-3}) were 0.84 Å from $Gd^{(1)}$ and 0.76 Å from $Gd^{(2)}$. The weighting scheme used during refinement is given in Table 2. Structure refinement and preparation of figures and tables for publication were carried out on PCs using SHELXTL/PC V5.1.[49] A complete list of atomic coordinates, bond lengths and angles, thermal parameters, and hydrogen atom coordinates are available from the Cambridge Crystallographic Data Centre. CCDC-213923 contains the supplementary crystallographic data for this paper. These data can be obtained free of charge at www.ccdc.cam.ac.uk/conts/retrieving.html [or from the Cambridge Crystallographic Data Centre, 12 Union Road, Cambridge CB2 1EZ, UK; Fax: (internat.) + 44-1223/336-033; E-mail: deposit@ccdc.cam.ac.uk].

Table 2. Crystal data and structure refinement for $[\{Na_{13}(OH)_3(H_2O)_{29}\}\{Gd^{(1)}(DOTP)\}][Gd^{(2)}(DOTP)]\cdot 7H_2O\cdot 2CH_3CH_2OH$

	Gd(DOTP)
Empirical formula	$C_{28}H_{133}Gd_2N_8Na_{13}O_{65}P_8$
Formula mass	2483.56
Temperature [K]	173(2)
λ(Mo-K_α) [Å]	0.71073
Crystal system	tetragonal
Space group	*P*4/*n*
a [Å]	16.4809(12)
b [Å]	16.4809(12)
c [Å]	21.989(2)
V [Å^3]	5972.7(9)
Z	4
$D_{calcd.}$ [g/cm^3]	1.381
μ [mm^{-1}]	1.342
F(000)	2536
Crystal size [mm]	0.49 × 0.44 × 0.10
θ range for data collection	2.23−28.30°
Index range	$-16 \le h \le 21$, $-20 \le k \le 21$, $-29 \le l \le 28$
Reflections collected	35498
Independent reflections	7042 [R(int) = 0.1124]
Max./min. transmission	0.8775/0.5594
Refinement method	full-matrix least squares on F^2
Data/restraints/parameters	7042/0/302
Goodness-of-fit on F^2	1.030
Final R indices [$I > 2\sigma(I)$]	R_1 = 0.1091[a], wR_2 = 0.2604[b]
R indices (all data)	R_1 = 0.1660[a], wR_2 = 0.2979[b]
Largest diff. peak and hole	3.976 and −1.571 e·Å^{-3}

[a] $R_1 = \Sigma||F_o| - |F_c||/\Sigma|F_o|$. [b] $wR_2 = \{\Sigma[w(||F_o|^2 - |F_c|^2|)^2]|/\Sigma[w(F_o^4)]\}^{1/2}$.

Acknowledgments

We thank Fundação da Ciência e Tecnologia (F.C.T.), Portugal (project POCTI/QUI/47005/2002), and Universidade da Coruña, Spain, for financial support, and the COST D18 Action of the E. U.

[1] A. D. Sherry, C. F. G. C. Geraldes, in: *Lanthanide Probes in Life, Chemical and Earth Sciences* (Eds.: J.-C. Bünzli, G. R. Choppin), Elsevier, Amsterdam, **1989**, pp. 93−126.
[2] R. B. Lauffer, *Chem. Rev.* **1987**, *87*, 901−927.
[3] M. F. Tweedle, in: *Lanthanide Probes in Life, Chemical and Earth Sciences* (Eds.: J.-C. Bünzli, G. R. Choppin), Elsevier, Amsterdam, **1989**, pp. 127−179.
[4] P. Caravan, J. J. Ellison, T. J. McMurry, R. B. Lauffer, *Chem. Rev.* **1999**, *99*, 2293−2352.
[5] [5a] S. Aime, M. Botta, M. Fasano, E. Terreno, *Chem. Soc. Rev.* **1998**, *27*, 19−29. [5b] S. Aime, M. Botta, M. Fasano, S. Geninnatti Crich, E. Terreno, *Coord. Chem. Rev.* **1999**, *185−186*, 321−333.
[6] A. D. Sherry, C. R. Malloy, F. M. H. Jeffrey, W. P. Cacheris, C. F. G. C. Geraldes, *J. Magn. Reson.* **1988**, *76*, 528−533.
[7] D. C. Buster, M. M. C. A. Castro, C. F. G. C. Geraldes, C. R. Malloy, A. D. Sherry, T. C. Siemers, *Magn. Reson. Med.* **1990**, *15*, 25−32.
[8] C. R. Malloy, D. C. Buster, M. M. C. A. Castro, C. F. G. C. Geraldes, F. M. H. Jeffrey, A. D. Sherry, *Magn. Reson. Med.* **1990**, *15*, 33−44.
[9] N. B. Butwell, R. Ramasamy, A. D. Sherry, C. R. Malloy, *Invest. Radiol.* **1991**, *26*, 1079−1082.
[10] N. B. Butwell, R. Ramasamy, I. Lazar, A. D. Sherry, C. R. Malloy, *Am. J. Physiol.* **1993**, *264*, H1884−H1889.
[11] M. M. Pike, C. Su Luo, M. D. Clark, K. A. Kirk, M. Kitakaze, M. C. Madden, E. J. Cragoe Jr., G. M. Pohost, *Am. J. Physiol.* **1993**, *265*, H2017−H2026.
[12] N. Bansal, M. J. Germann, I. Lazar, C. R. Malloy, A. D. Sherry, *J. Magn. Reson. Imag.* **1992**, *2*, 385−391.
[13] N. Bansal, M. J. Germann, V. Seshan, G. T. Shires III, C. R. Malloy, A. D. Sherry, *Biochemistry* **1993**, *32*, 5638−5643.
[14] Z.-F. Xia, J. W. Horton, P.-Y. Zhao, N. Bansal, E. E. Babcock, A. D. Sherry, C. R. Malloy, *J. Appl. Physiol.* **1994**, *76*, 1507−1511.
[15] V. Seshan, M. J. Germann, P. Preisig, C. R. Malloy, A. D. Sherry, N. Bansal, *Magn. Reson. Med.* **1995**, *34*, 25−32.
[16] J. D. Makos, C. R. Malloy, A. D. Sherry, *J. Appl. Physiol.* **1998**, *85*, 1800−1805.

[17] P. M. Winter, V. Seshan, J. D. Makos, A. D. Sherry, C. R. Malloy, N. Bansal, *J. Appl. Physiol.* **1998**, *85*, 1806−1812.
[18] C. F. G. C. Geraldes, R. D. Brown III, W. P. Cacheris, S. Koenig, A. D. Sherry, M. Spiller, *Magn. Res. Med.* **1989**, *9*, 94−104.
[19] S. Aime, M. Botta, E. Terreno, P. L. Anelli, F. Uggeri, *Magn. Res. Med.* **1993**, *30*, 583−591.
[20] S. Aime, M. Botta, D. Parker, J. A. G. Williams, *J. Chem. Soc., Dalton Trans.* **1996**, 17−23.
[21] A. D. Sherry, C. F. G. C. Geraldes, W. P. Cacheris, *Inorg. Chim. Acta* **1987**, *139*, 137−139.
[22] C. F. G. C. Geraldes, A. D. Sherry, G. E. Kiefer, *J. Magn. Reson.* **1992**, *97*, 290−304.
[23] J. Ren, A. D. Sherry, *J. Magn. Reson.* **1996**, *B111*, 178−182.
[24] S. Aime, M. Botta, E. Garino, S. G. Crich, G. B. Giovenzana, R. Pagliarin, G. Palmisano, M. Sisti, *Chem. Eur. J.* **2000**, *6*, 2609−2617.
[25] J. A. Peters, J. Huskens, D. J. Raber, *Prog. NMR Spectrosc.* **1996**, *28*, 283−350.
[26] J. A. Peters, E. Zitha-Bovens, D. M. Corsi, C. F. G. C. Geraldes, in: *The Chemistry of Contrast Agents in Medical Magnetic Resonance Imaging* (Eds.: A. E. Merbach, É. Tóth), John Wiley & Sons, Chichester, **2001**, chapter 8.
[27] E. F. Paulus, P. Juretschke, J. Lang, *3. Jahrestag der Deutschen Gesellschaft für Kristallographie*, Darmstadt, **1995**.
[28] A. D. Sherry, J. Ren, J. Huskens, E. Brücher, É. Tóth, C. F. G. C. Geraldes, M. M. C. A. Castro, W. P. Cacheris, *Inorg. Chem.* **1996**, *35*, 4604−4612.
[29] J. Ren, A. D. Sherry, *Inorg. Chim. Acta* **1996**, *246*, 331−341.
[30] [30a] C. Piguet, J.-C. G. Bünzli, G. Bernardinelli, C. G. Bochet, P. Froidevaux, *J. Chem. Soc., Dalton Trans.* **1995**, 83−97; M. Elhabiri, R. Scopelliti, J.-C. G. Bünzli, C. Piguet, *J. Am. Chem. Soc.* **1999**, *121*, 10747−10762. [30b] C. Platas, F. Avecilla, A. de Blas, T. Rodríguez-Blas, R. Bastida, A. Macías, A. Rodríguez, H. Adams, *J. Chem. Soc., Dalton Trans.* **2001**, 1699−1705.
[31] [31a] S. Aime, M. Botta, M. Fasano, M. P. M. Marques, C. F. G. C. Geraldes, D. Pubanz, A. E. Merbach, *Inorg. Chem.* **1997**, *36*, 2059−2068. [31b] S. Aime, A. Barge, F. Benetollo, G. Bombieri, M. Botta, F. Uggeri, *Inorg. Chem.* **1997**, *36*, 4287−4289.
[32] J. Ren, S. Zhang, A. D. Sherry, C. F. G. C. Geraldes, *Inorg. Chim. Acta* **2002**, *339C*, 273−282.
[33] J. Ren, C. S. Springer, A. D. Sherry, *Inorg. Chem.* **1997**, *36*, 3493−3498.
[34] S. Aime, M. Botta, S. G. Crich, E. Terreno, P. L. Anelli, F. Uggeri, *Chem. Eur. J.* **1999**, *5*, 1261−1266.
[35] D. M. Corsi, H. van Bekkum, J. A. Peters, *Inorg. Chem.* **2000**, *39*, 4802−4808.
[36] R. A. Carvalho, J. A. Peters, C. F. G. C. Geraldes, *Inorg. Chim. Acta* **1997**, *262*, 167−176.
[37] S. Aime, M. Botta, M. Fasano, S. G. Crich, E. Terreno, *J. Biol. Inorg. Chem.* **1996**, *1*, 312−319.
[38] L. Vander Elst, F. Maton, S. Laurent, F. Seghi, F. Chapelle, R. N. Muller, *Magn. Reson. Med.* **1997**, *38*, 604−614.
[39] R. B. Lauffer, D. J. Parmelee, S. U. Dunham, H. S. Ouellet, R. P. Dolan, S. Witte, T. J. McMurry, R. C. Walovitch, *Radiology* **1998**, *207*, 529−538.
[40] R. N. Muller, B. Radüchel, S. Laurent, J. Platzek, C. Piérart, P. Mareski, L. Vander Elst, *Eur. J. Inorg. Chem.* **1999**, 1949−1955.
[41] S. Aime, M. Chiaussa, G. Digilio, E. Gianolo, E. Terreno, *J. Biol. Inorg. Chem.* **1999**, *4*, 766−774.
[42] S. Aime, M. Botta, L. Frullano, S. G. Crich, G. B. Giovenzana, R. Pagliarin, G. Palmisano, M. Sisti, *Chem. Eur. J.* **1999**, *5*, 1253−1260.
[43] P. Caravan, M. T. Greenfield, X. Li, A. D. Sherry, *Inorg. Chem.* **2001**, *40*, 6580−6587.
[44] K. I. Hardcastle, M. Botta, M. Fasano, G. Digilio, *Eur. J. Inorg. Chem.* **2000**, 971−977.
[45] M. Botta, *Eur. J. Inorg. Chem.* **2000**, 399−407.
[46] [46a] É. Tóth, L. Helm, A. E. Merbach, in: *The Chemistry of Contrast Agents in Medical Magnetic Resonance Imaging* (Eds.: A. E. Merbach, É. Tóth), John Wiley & Sons, Chichester, England, **2001**, chapter 2, p. 45. [46b] D. H. Powell, O. M. N. Dhubhghaill, D. Pubanz, L. Helm, Y. S. Lebedev, W. Schlaepfer, A. E. Merbach, *J. Am. Chem. Soc.* **1996**, *118*, 9333−9346.
[47] S. Aime, A. S. Batsanov, M. Botta, J. A. K. Howard, D. Parker, K. Senanayake, G. Williams, *Inorg. Chem.* **1994**, *33*, 4696−4706.
[48] A. Borel, L. Helm, A. Merbach, *Chem. Eur. J.* **2001**, *7*, 600−610.
[49] G. M. Sheldrick, *SHELXTL: An Integrated System for Solving and Refining Crystal Structures from Diffraction Data (Revision 5.1)*, University of Göttingen, Germany, **1997**.

Received May 27, 2003
Early View Article
Published Online October 10, 2003

